A Letters Journal Exploring the Frontiers of Physics

October 2008

EPL, **84** (2008) 28003
doi: 10.1209/0295-5075/84/28003

www.epljournal.org

Short-time self-diffusion of weakly charged silica spheres at aqueous interfaces

Wei Chen and Penger Tong[a]

Department of Physics, Hong Kong University of Science and Technology - Clear Water Bay, Kowloon, Hong Kong

received 7 April 2008; accepted in final form 9 September 2008
published online 7 October 2008

PACS 82.70.Dd – Colloids
PACS 68.05.Gh – Interfacial properties of microemulsions
PACS 05.40.-a – Fluctuation phenomena, random processes, noise, and Brownian motion

Abstract – Optical microscopy and multi-particle tracking are used to study the short-time self-diffusion of weakly charged silica spheres at a water-air interface. The measured short-time self-diffusion coefficient D_S^S has the form, $D_S^S/D_0 = \alpha(1-\beta n)$, where n is the area fraction occupied by the particles and D_0 is the Stokes-Einstein diffusion coefficient of individual particles in the bulk fluid. The obtained values of α and β differ from those obtained for bulk suspensions, indicating that hydrodynamic interactions between the interfacial particles have interesting new features when compared with their three-dimensional counterpart.

A monolayer of colloidal particles suspended at a water-air (or water-oil) interface has served as a model system to study a range of important issues at soft (liquid-liquid) interfaces. Examples include two-dimensional (2D) ordering [1], crystallization [2] and aggregation [3], interactions between similarly charged particles [4,5], and dislocation boundaries of a colloidal crystal ball [6]. These studies focused on the equilibrium properties of the interfacial particles. Colloidal particles have also been used as tracer particles to study the rheological properties of soft interfaces. For example, Sickert and Rondelez [7] measured the Brownian diffusion coefficient of $0.4\,\mu$m diameter polystyrene beads immersed in a monolayer of surfactant molecules at a water-air interface. Prasad *et al.* [8] extended the single-particle method to two-particle microrheology by measuring the relative diffusion between two micron-sized polystyrene beads suspended at a protein-coated water-air interface.

While these measurements revealed interesting new features of tracer diffusion in macromolecular films, interpretation of the experimental results is not straightforward [9,10]. The measured diffusion coefficient is inversely proportional to the drag coefficient felt by the interfacial particles. The theoretical calculations, which connect the measured drag coefficient to the surface rheological properties of interest, such as the surface shear viscosity η_s, consider idealized situations, whereas the actual systems used in the experiment often reveal interesting but unexpected deviations. Therefore, direct measurements of particle's diffusion coefficient at interfaces without a surfactant monolayer are needed as the first step to verify the theoretical models for interfacial diffusion [10–12].

Compared to the large number of experimental (and theoretical) studies of colloidal dynamics in 3D suspensions [13], systematic experimental studies of colloidal diffusion at interfaces are rather limited. The lack of progress is partially due to a lack of well-controlled 2D colloidal systems for the experimental studies. Early experiments on colloidal diffusion at liquid-air interfaces [7,11] were carried out only for a few particles. Because of the limited statistics, the measured diffusion coefficient suffered large experimental uncertainties, making it difficult to quantitatively compare with the theoretical predictions [9,10,14]. In the experiment, polystyrene (PS) latex spheres are often used as tracer particles. The PS spheres are highly charged and show a strong dipole repulsion when dispersed at the interface [2,5,15]. The strong long-ranged repulsion could affect the diffusion measurement at the interface.

The interactions and dynamics of colloidal particles are known to be sensitive to weak forces (of order pico- or femto-Newtons). This sensitivity is further magnified at interfaces. As a result, the stability of interfacial particles becomes extremely sensitive to impurities at the interface [16]. Accurate measurements of particle motion require well-controlled procedures to thoroughly clean the

[a] E-mail: penger@ust.hk

Table 1: Particle samples used in the experiment and the fitted value of the parameters in the linear fit: $D_S^S/D_0 = \alpha(1-\beta n)$. The numbers in the parentheses are obtained from the second-order polynomial fit: $D_S^S/D_0 = \alpha(1-\beta n-\gamma n^2)$.

Sample/Manu.	d (μm)	α ($\pm 7\%$)	β ($\pm 10\%$)	γ ($\pm 15\%$)
Si2/Duke Sci.	1.57 ± 0.06	1.19 (1.17)	1.6 (0.84)	(5.56)
Si3/Bangs Lab	0.97 ± 0.05	1.45 (1.45)	1.84 (1.53)	(6.61)
Si1/Duke Sci.	0.73 ± 0.04	1.18 (1.17)	2.89 (2.44)	(5.75)

interface and colloidal samples, so that a well-dispersed monolayer of particles can be routinely made at the interface. Unstable particles form colloidal aggregates or clusters at the interface, making the measurement of individual particle motion inaccurate or impossible at all if there are too many colloidal aggregates present in the sample. In a recent experiment [5], we developed the experimental procedures necessary to produce such a monolayer of colloidal particles. With the well-controlled 2D colloidal systems, one can carry out precise measurements of the particles' diffusion coefficient at different interfaces.

In this letter, we report key results of a systematic experimental study of short-time self-diffusion of weakly charged silica spheres at a water-air interface. As will be shown below, this is a model 2D system in which the silica spheres interact via a short-range repulsion. In the experiment, we measure the mean squared displacement (MSD) of a diffusing particle,

$$\langle \Delta \mathbf{r}^2(\tau) \rangle = (1/N) \sum_i \langle |\mathbf{r}_i(t+\tau) - \mathbf{r}_i(t)|^2 \rangle_t, \qquad (1)$$

as a function of lag time τ. Here $\mathbf{r}_i(t)$ is the position of the i-th particle at time t, N is the number of particles included in the calculation, and the angle brackets $\langle \ldots \rangle_t$ indicate an average over t.

The diffusion of particles is characterized by two distinct regimes. For low surface coverage and times much less than the time, $t_0 = d^2/D_0$, for a particle to diffuse over its own diameter d, the particle's motion is not hindered by direct interactions with neighboring particles and only the hydrodynamic interactions with the surrounding fluid are important. Here $D_0 = k_B T/(3\pi\eta d)$ is the Stokes-Einstein diffusion coefficient for a single particle with thermal energy $k_B T$ fully immersed in a liquid of viscosity η. At long times ($\tau \gg t_0$), however, the particle's motion is impeded by direct interactions with neighboring particles and thus the self-diffusion is affected by both direct and hydrodynamic interactions. While the above arguments were given originally for bulk diffusion of hard spheres [17], we believe they are also applicable to interfacial diffusion except that two minor changes are needed. First, for particles with a short interaction range, $\widetilde{d}$ ($> d$), the hard-sphere diameter d should be replaced by $\widetilde{d}$. Second, for particles at a liquid-air interface, their hydrodynamic drag is reduced, leading to a larger D_0 compared with the bulk suspension. For silica spheres at the water-air interface, the two competing effects give rise to a modified t_0, which is approximately 50% larger than that for the bulk suspension.

Here we focus on the new measurements of the short-time self-diffusion coefficient $D_S^S(n)$ as a function of area fraction, $n = \pi a^2 \aleph/A$, occupied by the interfacial particles, where $\aleph$ is the total number of particles in the area A. We follow the same procedures as described in ref. [5] for the experimental setup and the sample preparation and cleaning. The sample cell is made from a stainless-steel disk (which is hydrophilic) with a central hole of diameter 13 mm. The bottom of the hole is sealed with a 0.1 mm thick glass cover slip, which also serves as an optical window. The sidewall of the hole together with the bottom glass slip forms a container, which has an effective height of 1.0 mm. The top of the container has a sharp circular edge, which is used to pin the water-air interface and reduce unwanted surface flow. The entire cell is placed on the sample stage of an inverted microscope, so that the motion of the interfacial particles can be viewed from below and recorded by a digital camera.

Table 1 gives the value of the diameter d and the manufacturer of three silica particle samples used in the experiment. Dynamic light scattering [18] is used to measure the bulk diffusion coefficient D_0 in water for each particle sample. The final results agree well with the calculated D_0. Great care is taken to clean the particle samples and the water-air interface. Surface pressure measurements reveal that no detectable impurity is found in the cleaned particle samples. The particle-methanol solution is then injected onto a cleaned interface using a syringe pump. The silica spheres disperse well at the clean water-air interface. Individual particles undergo vigorous Brownian motion and remain stable at the interface for days.

These particles remain in focus under high magnification, indicating that the silica spheres are strongly bound to the interface and their vertical position is determined by an energy minimum, much larger than $k_B T$, that keeps them at the interface [2]. Because the gravitational energy of the particles is much smaller than the relevant energy of the interface, the particles can always choose an equilibrium (vertical) position without introducing long-range deformations to the interface. Therefore, the usual capillary effect is not applicable to micron-sized spheres. Using an estimated contact angle of 60° [19], we find approximately 3/4 of the silica particle (by diameter) is immersed in water.

Phase contrast microscopy is used to obtain good images of the silica particles. The particle trajectories are constructed from the consecutive images using homemade software with a spatial resolution of 60–100 nm. Typically,

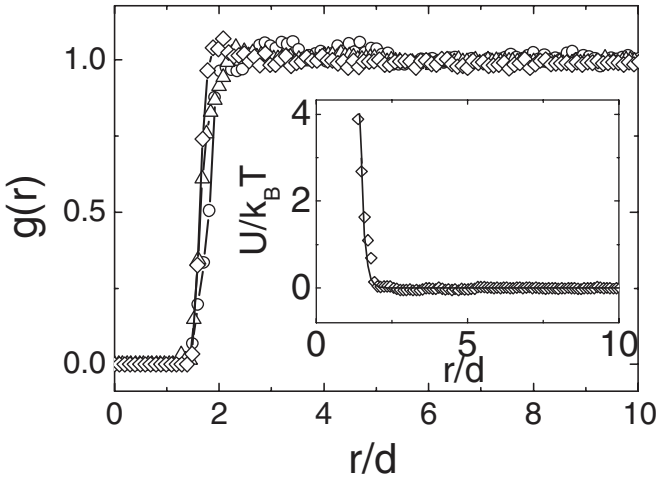

Fig. 1: Measured pair correlation function $g(r)$ as a function of r/d for Si1 (circles), Si2 (diamonds), and Si3 (triangles). All the measurements are made at the same area fraction $n = 0.018$. Insert shows the interaction potential $U(r)/k_BT$ *vs.* r/d obtained from the measured $g(r)$ for Si2. The solid curve shows a least-square fit to the screened Coulomb potential (see text).

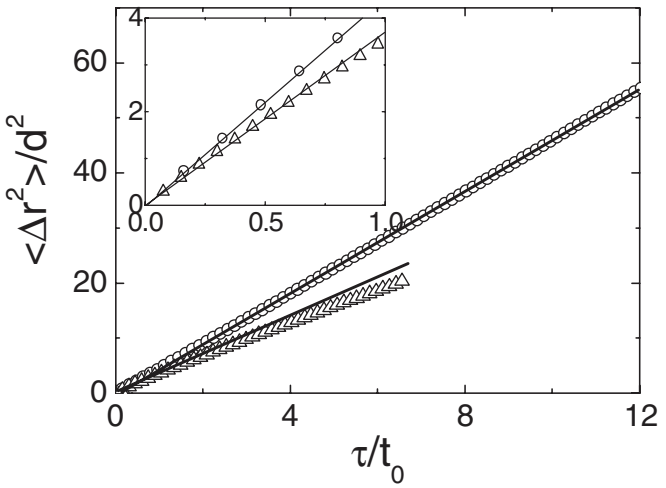

Fig. 2: Normalized mean-squared displacement $\langle \Delta \mathbf{r}^2(\tau)\rangle/d^2$ as a function of τ/t_0 for Si1 at $n = 0.01$ (circles) and $n = 0.09$ (triangles). The solid lines show the linear fits to the data points (at small τ for the lower curve). Insert shows a magnified plot of the same data for $\tau/t_0 < 1.0$.

we use 10 image sequences, each contains 100 images, to calculate MSD, and the result is further averaged over repeated runs (10–20 runs). This corresponds to an average over 10^6 particles, ensuring that the statistical averaging is adequate. Using the same image data, we also calculate the pair correlation function $g(r)$ [5].

Figure 1 shows the obtained $g(r)$ for three silica samples at low surface coverage. The measured pair correlation functions overlap rather well once the inter-particle distance r is scaled by d. Silica spheres represent an important class of charged particles commonly used in colloidal science and have anionic SiO^- groups on their surface [20,21]. These charged spheres at the interface show a short-range repulsion with an effective hard-sphere diameter $\widetilde{d} \simeq 1.5d$, in which $g(r) \simeq 0$. This value is about one-half of the mean particle separation, $\ell = d[\pi/(4n)]^{1/2} \simeq 2.8d$, for $n = 0.1$.

When the surface coverage is small ($n \lesssim 0.018$), many-body corrections to $g(r)$ are negligible [5] and the phase interaction potential $U(r)$ can be obtained via the Boltzmann factor $g(r) \simeq \exp[-U(r)/k_BT]$. Insert of fig. 1 shows the resulting $U(r)/k_BT$, which can be well described by the screened Coulomb potential,

$$U_c(r) = \frac{q^2 \exp[-(r-d)/\lambda_D]}{4\pi\epsilon_0\epsilon[1+d/(2\lambda_D)]^2 r}. \qquad (2)$$

The solid line shows a fit with the effective charge $q = (3300 \pm 900)e$ and the screening length $\lambda_D = (204 \pm 20)$ nm. The fitting results are consistent with those obtained previously for the bulk suspension of silica spheres [20]. The surface charge density corresponding to this value of q is ~ 200 times smaller than that of the polystyrene latex spheres [5].

In a separate experiment [22], we systematically studied the effect of adding salt (NaCl) on the interaction between silica spheres at the water-air interface. For the interface made of fresh deionized water (the present experiment uses fresh deionized water too), the potential $U(r)$ was found to be dominated by the screened Coulomb repulsion shown in eq. (2). Weaker forces at one or two particle diameters away show up only when λ_D becomes smaller than 100 nm (*i.e.,* when the salt concentration $C \gtrsim 10\,\mu$M). The maximum amplitude of these weaker interactions is less than $0.3\,k_BT$. In particular, the amplitude of the long-ranged electric-dipole repulsion mentioned above is less than 0.1 k_BT, which is too small to affect the measured $D_S^S(n)$ to be presented below.

Figure 2 shows the measured $\langle \Delta \mathbf{r}^2(\tau)\rangle$ as a function of τ for Si1 at $n = 0.01$ (circles) and $n = 0.09$ (triangles). The data are plotted in dimensionless units with $\langle \Delta \mathbf{r}^2(\tau)\rangle$ scaled by d^2 and τ scaled by t_0. For low-concentration samples ($n \lesssim 0.05$), we find the measured $\langle \Delta \mathbf{r}^2(\tau)\rangle$ is a linear function of τ over the entire range of τ, indicating that the particles are undergoing free diffusion. For higher concentration samples, however, the measured $\langle \Delta \mathbf{r}^2(\tau)\rangle$ curves down slightly, as shown by the lower curve in fig. 2. This downward curving effect becomes more pronounced when $n \gtrsim 0.1$.

Figure 3 shows the equilibrium configuration of silica spheres (Si1) at two area fractions. As mentioned above, the mean particle separation (center-to-center) is $\ell \simeq 2.8d$ when $n \simeq 0.1$, indicating that the probability for a tracer particle to encounter a neighboring particle when it diffuses over its own diameter d (or over a time period t_0) is low. Therefore, one expects that the Brownian motion of the interfacial particles will not be hindered when $\tau \lesssim t_0$. Indeed, insert of fig. 2 shows that

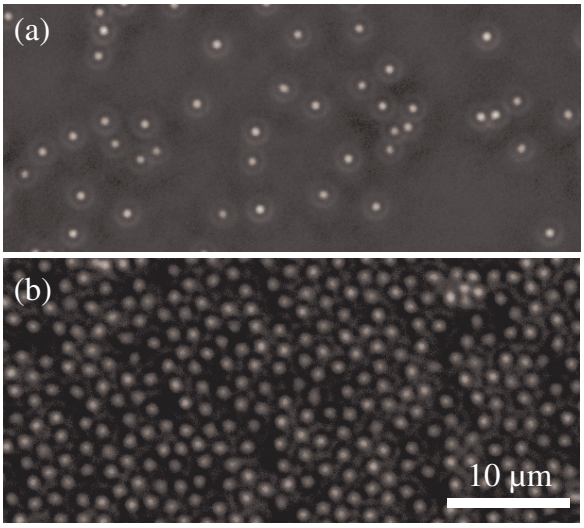

Fig. 3: Equilibrium configurations of the silica spheres (Si1) at (a) low surface coverage ($n \simeq 0.01$) and (b) high surface coverage ($n \simeq 0.12$).

the measured $\langle \Delta \mathbf{r}^2(\tau) \rangle$ remains the linear dependence on τ when $\tau/t_0 \lesssim 1$. A similar behavior is also observed for other silica samples.

From the initial slope of the linear fit (solid lines shown in insert of fig. 2), we obtain the normalized short-time self-diffusion coefficient D_S^S/D_0 via the equation $\langle \Delta \mathbf{r}^2(\tau) \rangle / d^2 = 4(D_S^S/D_0)(\tau/t_0)$. Figure 4 shows how the measured $D_S^S(n)/D_0$ changes with n for Si1 (circles in fig. 4(a)), Si2 (triangles in fig. 4(a)) and Si3 (circles in fig. 4(b)). All the measured D_S^S/D_0 follows the same trend that it decreases with increasing n. At low surface coverage ($n \lesssim 0.1$), the measured D_S^S/D_0 can be fit to a linear function,

$$\frac{D_S^S}{D_0} = \alpha(1 - \beta n), \tag{3}$$

with the fitted values of α and β given in table 1. The standard deviations for α are typically 7% and those for β are 10%. The experimental uncertainties for α are mainly from statistical errors. The relatively larger uncertainties for β are caused in part by the fact that the fitted β also varies with the range of n chosen for the linear fit.

The dashed curves in fig. 4 show the second-order polynomial fit, $D_S^S/D_0 = \alpha(1 - \beta n - \gamma n^2)$, to the data points over the entire range of n. The fitted values of α, β and γ are also included in table 1. The values of β obtained from the second-order polynomial fit are somewhat smaller than those obtained from the linear fit. It is of interest to note that the second-order term is negative for all the particle samples and its absolute value depends non-monotonically on the size of the particles. Because three-body interactions are involved in the second-order term, the fitted values of γ are expected to be more sensitive to the details of hydrodynamic interactions at the interface.

Figure 4 reveals two novel features of interfacial hydrodynamics. First, at the single particle level, the measured

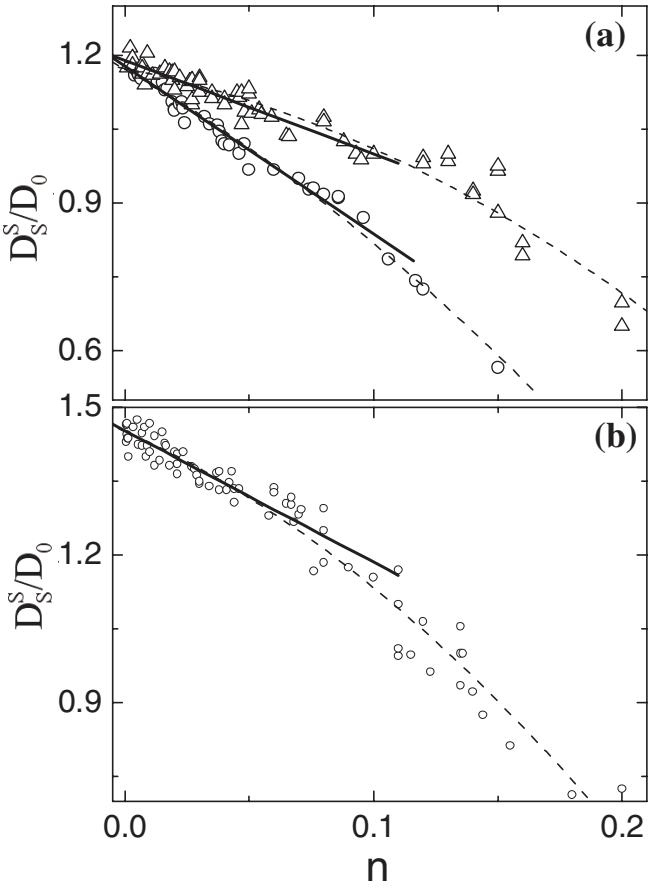

Fig. 4: (a) Normalized short-time self-diffusion coefficient D_S^S/D_0 as a function of area fraction n for three silica samples: (a) Si1 (circles), Si2 (triangles) and (b) Si3 (circles). The solid lines show the linear fits to the data points with $n < 0.1$. The dashed curves are the second-order polynomial fits, $D_S^S/D_0 = 1.17 - 0.98n - 6.51n^2$ (upper dashed curve in (a)), $D_S^S/D_0 = 1.17 - 2.86n - 6.73n^2$ (lower dashed curve in (a)), and $D_S^S/D_0 = 1.45 - 2.22n - 9.58n^2$ (dashed curve in (b)), to the data points over the entire range of n.

D_S^S at the $n \to 0$ limit is directly related to the drag coefficient ξ via the equation $D_S^S(n=0) = k_B T/\xi$. For interfacial particles, one finds [12]

$$\xi = (\eta_1 a) f(z/a, B), \tag{4}$$

where z is the distance between the sphere's north pole and the interface (*i.e.,* $z = 0$ when the sphere is in contact with the interface from below). The Boussinesq number B is defined as $B = \eta_s/[(\eta_1 + \eta_2)a]$, where η_s is the shear viscosity of the interface and η_1 and η_2 are, respectively, the viscosities of the lower and upper phase fluids forming the interface. For a water-air interface, one has $\eta_2 \simeq 0$. The correction factor $f(z/a, B)$ accounts for all the effects of the interfacial hydrodynamics at the single-particle level and thus is a key quantity for understanding the rheological properties of liquid-liquid interfaces.

Because the water-air interface is thoroughly cleaned, we expect the Boussinesq number B to be small in our

case. Therefore, one has [12] $f(z/a, 0) = k^{(0)}$, where $k^{(0)}$ is the zeroth-order correction factor and is determined solely by z/a. The numerically calculated $k^{(0)}$ in ref. [12] for the liquid-air interface is an increasing function of z/a from the minimum value of $k^{(0)} = 0$ at $z/a = -2$ to the maximum value of $k^{(0)} \simeq 0.7856(6\pi) \simeq 14.81$ at $z/a = 0$. For particles fully immersed in water ($z/a \to \infty$ limit), one has $k^{(0)} = 6\pi$.

From eqs. (3) and (4), one finds the measured value of $k^{(0)}$ is $6\pi/\alpha$. By comparing the measured value of $k^{(0)} \simeq 13.0$ for Si3 with the calculated $k^{(0)}$ as a function of z/a in ref. [12], we find that the vertical position of Si3 spheres is located at $z/a \simeq -0.564$. The contact angle corresponding to this vertical position is $\theta = \cos^{-1}(1 - |z/a|) \simeq 64.1°$, which is very close to the independently measured value of $\theta \simeq 60°$ [19]. The experiment thus demonstrates that the measured single-particle self-diffusion together with the calculated $k^{(0)}$ can provide a useful technique to determine the contact angle of well-behaved colloidal particles at the interface.

The obtained value of $k^{(0)} \simeq 15.97$ for Si1 and Si2 is $\sim 7.9\%$ larger than the maximum value allowed, suggesting that these silica spheres experience a larger drag force at the interface. The discrepancy between the measurement and theory is beyond the experimental uncertainties. What causes these particles to feel larger drag force at the interface? One possibility is due to surface contaminations, which are known to hinder the motion of interfacial particles [5,16]. However, such effect is expected to be random, but our measurements show consistent results for all three particle samples. In the experiment, great care is taken to clean the interface and the fitted value of α for each particle sample is extrapolated from 20–30 independent measurements conducted at different times with separately prepared water-air interfaces. The measurements with different particle samples thus indicate that the larger drag forces experienced by Si1 and Si2 are unlikely caused by surface contaminations.

Another possibility is that the difference in surface chemistry between Si3 and Si1 (or Si2) may introduce additional drag forces due to the pining of the interface or meniscus deformation in the immediate vicinity of the contact line between the interface and particle. The numerical calculation by Fischer *et al.* [12] assumed that the interface is flat and incompressible but did not consider any complication near the contact line. The Si3 particles were purchased from Bangs Laboratories and are non-porous silica spheres. These non-porous particles show the normal behavior of interfacial diffusion and sit on the interface with the expected value of z/a (or contact angle). The Si1 and Si2 particles were purchased from Duke Scientific and were synthesized by the Stöber method, followed by a sintering process at 900 °C to drive off all organic materials and water [23]. The Stöber silica is known to be somewhat porous [21], which may introduce meniscus deformation or interface pining near the contact line.

The third possibility is that the Si1 (or Si2) particles may immerse into the water deeper than a flat interface allows but still remain in contact with the (curved) interface [24]. As a rough estimate, we take the calculated value of $k^{(0)}$ to be 15.97 and find the corresponding value of $z/a \simeq 0.5$ from ref. [12]. This estimation suggests that the measured $k^{(0)} \simeq 15.97$ could be accounted for if the particles dip into the water by a quarter of its own diameter deeper than a flat interface allows. While at the moment we do not know exactly what would cause such dipping, the electric-field–induced capillary effect [25] could be a candidate for this phenomenon. Because of the large difference in dielectric constant across the interface, there is an inhomogeneous pressure exerted on the interface, resulting in an effective force pulling the particle into the water. Clearly, a further understanding of the interaction between the particle surface and the interface is an important issue, which affects a range of problems associated with tracer diffusion at soft interfaces [10–12,26].

The second new feature shown in fig. 4 is that the measured $D_S^S(n)$ shows an interesting concentration dependence, which is directly related to interfacial hydrodynamic interactions between the particles. The fitted values of β for the three silica samples are not the same, with the larger particles having a smaller value of β. The difference between the fitted values of β is clearly beyond the experimental uncertainties. The extra d-dependence of the measured β suggests that smaller particles experience a larger resistance (dissipation) than larger particles. Such an effect was also observed in a different colloidal monolayer system consisting of nearly hard spheres (polymethylmethacrylate (PMMA) particles) at a decalin-water interface with a contact angle close to 180° [27]. Peng *et al.* found that the fitted values of β for two PMMA samples of different sizes also decrease with increasing d. These results indicate that the additional d-dependence of the measured D_S^S/D_0 is a general feature of interfacial diffusion. An intriguing question arising from the above observations is: What causes the d-dependence of the measured β? Currently, there is no analytical theory or numerical simulation available to explain the effect. From the experimental point of view, there are several candidates which may explain why large and small particles feel different hydrodynamic interactions at the interface.

One possibility is that the large and small particles may have slightly different wetting conditions at the interface. For example, larger particles are bound more strongly to the interface than smaller particles. In the experiment, we also found that it gets increasingly difficulty to disperse small particles ($< 0.4\,\mu$m) at the interface. Figure 1 showed that the three silica particles experience a repulsive interaction with minute differences. The short-range repulsion could increase the effective area fraction n, making the value of the effective β smaller. This issue of interaction is further complicated if one considers that the silica spheres are weakly charged and the counter-ions are distributed

in the immediate vicinity of the particle surface in contact with the water. While these effects may be very small for the equilibrium properties of the colloidal monolayer, such as the pair correlation function and the contact angle, the dynamic properties of the monolayer, such as the measured D_S^S, could be more sensitive to these small variations. As mentioned above, because the relevant surface energy is large, a small change in contact area may result in a large change in the surface energy (and hence the dissipation), much larger than k_BT. Another possibility comes from possible surface contaminations. While we have tried the best we could to clean the interface, we do not have direct knowledge of whether our cleaning is perfect. Non-perfect cleaning may give rise to a non-zero Boussinesq number B, providing another channel for viscous dissipation (or drag).

For bulk suspensions, it was found [17] that $D_S^S/D_0 = 1-\beta_3\phi$, where ϕ is the volume fraction of particles and the coefficient $\beta_3 \simeq 1.83$ is independent of d. The measured value of β_3 agrees well with the theory of two-body hydrodynamic interactions in the bulk suspension [13,17]. One may have a simple estimate of β_3 by examining the concentration dependence of the effective viscosity, $\eta_{eff} = \eta(1+\beta_3'\phi)$, of the suspension, where η is the solvent viscosity. Assuming $\xi \simeq 6\pi\eta_{eff}a$, one obtains $D_S^S/D_0 \propto (1-\beta_3'\phi)$. Einstein showed $\beta_3' = 5/2$ [28], which is slightly larger than the measured $\beta_3 \simeq 1.83$. This is because the concept of effective viscosity applies only to the situation for one big tracer particle in a suspension of many small particles. By contrast, D_S^S is measured with one tracer particle in a bath of many particles of the same size. The local viscosity felt by smaller tracer particles is less than that felt by bigger tracer particles [29].

Compared with the bulk suspensions, hydrodynamic interactions between interfacial particles are much less understood. At the moment, we are not aware of any theoretical calculation for β at the interface. The motion of the colloidal monolayer is complicated because it is a coupled system of the interface with the lower fluid phase. If the Boussinesq number B is large enough, the effective viscosity, $\eta_{eff} = \eta(1+\beta_2 n)$, of a 2D colloidal system is increased with $\beta_2 = 4$ [30]. Because smaller particles are separated by a smaller distance ($\ell = d[\pi/(4n)]^{1/2}$) as compared to the larger particles at the same area fraction n, they may feel more 2D-like hydrodynamic interactions than the larger particles do [30,31]. This could explain why small particles experience more hydrodynamic resistance (drag) with increasing surface concentrations. Clearly, a detailed calculation of two-body hydrodynamic interactions at the interface is needed in order to further understand the concentration dependence of the measured $D_S^S(n)$.

* * *

We have benefited from illuminating discussions and correspondence with T. Fischer and are indebted to W. Ford, H. Stone, M. Brenner, D. Weitz, B. Ackerson, T. Squires, A. Levine and T. K. Ng for useful discussions. This work was supported by the Research Grants Council of Hong Kong SAR under Grant No. HKUST602806.

REFERENCES

[1] Onada G. Y., *Phys. Rev. Lett.*, **55** (1985) 226.
[2] Pieranski P., *Phys. Rev. Lett.*, **45** (1980) 569; Hurd A. J., *J. Phys. A*, **18** (1985) L1055.
[3] Hurd A. J. and Shaefer D. W., *Phys. Rev. Lett.*, **54** (1985) 1043.
[4] Ruiz-Garcia J. *et al.*, *Phys. Rev. E*, **58** (1998) 660; Nikolaides M. G. *et al.*, *Nature*, **420** (2002) 299.
[5] Chen W. *et al.*, *Phys. Rev. Lett.*, **95** (2005) 218301; *Phys. Rev. E*, **74** (2006) 021406.
[6] Bausch A. R. *et al.*, *Science*, **299** (2002) 1716; Lipowsky *et al.*, *Nat. Mater.*, **4** (2005) 407.
[7] Sickert M. and Rondelez F., *Phys. Rev. Lett.*, **90** (2003) 126104.
[8] Prasad V. *et al.*, *Phys. Rev. Lett.*, **97** (2006) 176001.
[9] Fischer T. M., *Phys. Rev. Lett.*, **92** (2004) 139603.
[10] Sickert M. and Rondelez F., *Phys. Rev. Lett.*, **92** (2004) 139604; Sickert M. *et al.*, *Europhys. Lett.*, **79** (2007) 66005; Stone H. A., preprint (2007).
[11] Radoev B. *et al.*, *Langmuir*, **8** (1992) 2962.
[12] Fischer T. M. *et al.*, *J. Fluid Mech.*, **558** (2006) 451.
[13] Pusey P. N., in *Liquids, Freezing and Glass Transition*, edited by Hansen J.-P. *et al.* (North-Holland, Amsterdam) 1991, Chapt. 10.
[14] Danov K. *et al.*, *J. Colloid Interface Sci.*, **175** (1995) 36; *Phys. Fluids*, **12** (2000) 2711.
[15] Aveyard R. *et al.*, *Phys. Rev. Lett.*, **88** (2002) 246102.
[16] Fernandez-Toledano J. C. *et al.*, *Langmuir*, **20** (2004) 6977.
[17] Qiu X. *et al.*, *Phys. Rev. Lett.*, **65** (1990) 516; van Blaaderen A. *et al.*, *J. Chem. Phys.*, **96** (1992) 4591; Segre P. N. *et al.*, *Phys. Rev. E*, **52** (1995) 5070.
[18] Berne B. J. and Pecora R., *Dynamic Light Scatttering* (Wiley, New York) 1976.
[19] Tolnai G. *et al.*, *J. Phys. Chem. B*, **107** (2003) 11109.
[20] Behrens S. H. and Grier D. G., *J. Chem. Phys.*, **115** (2001) 6716.
[21] Iler R. K., *The Chemistry of Silica* (Wiley & Sons, New York) 1979.
[22] Chen W. *et al.*, unpublished.
[23] Ford W., private communication.
[24] Fischer T. M., private communication.
[25] Foret L. and Würger A., *Phys. Rev. Lett.*, **92** (2004) 058302; Oettel M. *et al.*, *Phys. Rev. E*, **71** (2005) 051401.
[26] Saffman P. G. and Delebruck M., *Proc. Natl. Acad. Sci. U.S.A.*, **72** (1975) 3111.
[27] Peng Y. *et al.*, to be published in *J. Fluid Mech.*
[28] Russel W. B. *et al.*, *Colloidal Dispersion* (Cambridge University Press, Cambridge, UK) 1989.
[29] Tong P. *et al.*, *Phys. Rev. Lett.*, **79** (1997) 2362; Ye X. *et al.*, *Macromolecules*, **31** (1998) 5785.
[30] Khattari Z. *et al.*, *J. Phys. Chem. B*, **109** (2005) 3402.
[31] Fischer T. M., *J. Fluid Mech.*, **498** (2004) 123; Levine A. J. *et al.*, *Phys. Rev. E*, **66** (2002) 061606.